Strain rate imaging: fundamental principles and progress so far

Echocardiography remains the modality of choice for diagnosing heart disease in routine clinical practice. However, to date, the clinical approaches to evaluate regional myocardial function remain subjective and relatively poorly reproducible. As such, new ultrasound methodologies have been proposed in recent years in order to make this evaluation more quantitative and robust. This article reviews the technical principles behind these approaches as well as the clinical evidence that is already available showing the applicability and usefulness of these methodologies in daily clinical practice.

KEYWORDS: cardiac ▪ mechanics ▪ quantitative ▪ regional function ▪ strain ▪ strain rate ▪ ultrasound

Ruta Jasaityte[1] & Jan D'hooge[†1]

[1]Cardiovascular Imaging & Dynamics, Department of Cardiovascular Diseases, Catholic University of Leuven, Leuven, Belgium
[†]Author for correspondence:
Tel.: +321 634 9012; +321 634 3472
Fax: +321 634 3467
jan.dhooge@uz.kuleuven.be

Amongst the available imaging modalities echocardiography remains the modality of choice to diagnose heart disease in routine clinical practice due to its low cost, high temporal resolution, non-ionizing radiation and bedside applicability. In a typical ultrasound examination, a combination of cross-sectional (B-mode) images of the heart will be used to characterize the (regional) morphology of the heart and large vessels (FIGURE 1). In addition, as B-mode images can be generated in real-time, they can also be used to study and quantify cardiac dynamics in order to assess cardiac ejection performance. Finally, Doppler echocardiography allows visualization of the motion of blood within the heart and has, as such, become an indispensable tool for characterization of filling properties of the heart (FIGURE 2).

In spite of the widespread use of echocardiography a major challenge remains: an objective evaluation of regional myocardial function. Indeed, regional cardiac function is currently assessed semiquantitatively through visual wall motion scoring ('0' being normal kinetic to '3' being completely dyskinetic, i.e., moving in the opposite direction). Obviously, such a visual approach is strongly operator-dependent and therefore suffers from a high inter- and even intra-observer variability [1,2]. In this context, new echocardiographic tools have been introduced in recent years in order to make the assessment of regional myocardial function truly quantitative.

Originally, the echocardiographic Doppler system was modified in order to visualize the velocity profile of the myocardium rather than that of the blood [3]. Although this allowed quantifying motion characteristics of specific cardiac segments, the major problem arose from the fact that neighboring segments intrinsically influence each other's motion (an effect referred to in literature as 'tethering') [4]. Indeed, if one segment contracts the neighboring segments can be dragged along and therefore move without active contraction. As a result, the absolute value of the regional myocardial velocity does not necessarily represent the underlying myocardial performance. Moreover, there is a large variability in both the velocity amplitude and the velocity profile across the heart. For these reasons, as a natural next step, researchers suggested looking at the differences in velocities between myocardial segments (i.e., spatial velocity gradients) [4]. As such, myocardial deformation imaging was born, in which segmental myocardial deformation properties are noninvasively characterized.

In this article the essential concepts for a good understanding of myocardial deformation imaging are reviewed. First, the normal myocardial deformation characteristics are described based on knowledge from basic cardiac physiology. Then, a brief summary of different technical approaches for measuring myocardial deformation is given together with a discussion of their accuracy and their respective strengths and weaknesses. Finally, an overview is given of the clinical applications in which these techniques have already shown relevance.

Physiology of normal cardiac deformation characteristics
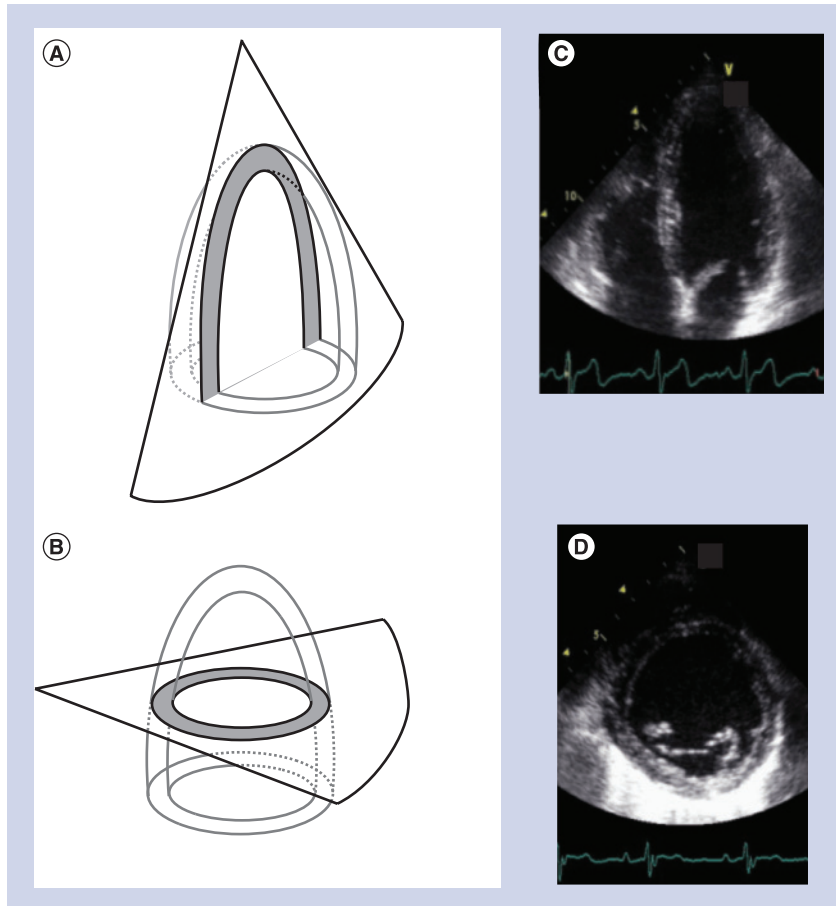
■ The cardiac cycle

The heart is a unique organ in the sense that it constantly undergoes contraction and

part of future medicine fsg

Figure 1. Schematic illustrations and ultrasound images of the left ventricle. Apical **(A)** and parasternal short axis **(B)** cross-sectional ultrasound images of the left ventricle are illustrated, alongside their corresponding clinical images **(C)** and **(D)**, respectively.

Figure 2. Left ventricular filling. Position of the pulsed wave Doppler sample **(A)**, resulting in a Doppler signal of the mitral inflow velocities, which shows the early and atrial left ventricular filling phases **(B)**. Color Doppler image of the left ventricular inflow tract **(C)**.

relaxation in a cyclic manner. The cardiac cycle can be divided into systole, during which ventricular muscle fibers (i.e., sarcomeres) contract (i.e., shorten), and diastole, during which sarcomeres relax (i.e., lengthen). The systolic contraction is associated with a reduction in cardiac chamber volume, which results in blood being ejected into the circulation. On the other hand, during diastole the ventricular chamber volume is restored as blood flows from the atrium to the ventricle.

Ventricular systole begins after the electrical depolarization (represented by the QRS complex in the ECG) with the isovolumic contraction during which the sarcomeres shorten and the intraventricular pressure increases rapidly at a constant ventricular volume (see phase B in Figure 3). When the intraventricular pressure exceeds the aortic pressure the aortic valve opens and the ejection period begins: the sarcomeres shorten further, the blood flows to the aorta and the ventricular volume decreases (see phase C in Figure 3). During these periods, the ventricle twists around its long axis (i.e., the basal and apical short axis slices rotate in opposite directions) due to the complex fiber structure. This twisting of the ventricle amplifies ejection and is thought to be associated with storage of potential energy. Ejection ends by aortic valve closure. Diastole then begins with the isovolumic relaxation, during which the intraventricular pressure falls rapidly at a constant ventricular volume until it becomes lower than the left atrial pressure and the mitral valve opens (see phase D in Figure 3). During this period, most of the ventricular untwisting occurs, which is consequently a relatively fast event, facilitated by a rapid release of potential energy stored during systolic twisting. After the mitral valve opening the rapid ventricular filling due to the pressure gradient between ventricle and atrium begins: the ventricular sarcomeres lengthen and ventricular volume increases (see phase E1 in Figure 3). When the pressure between the ventricle and atrium equalizes there is little or no flow of blood and minimal or no lengthening of the sarcomeres (see phase E2 in Figure 3). This phase of diastole is called diastasis. During the last phase of diastole the atrium contracts. As such, the atrial pressure exceeds the ventricular one and blood is forced to flow from the atrium to the ventricle (see phase A in Figure 3). The ventricular sarcomeres thus show lengthening (i.e., prestretch) and the ventricular volume increases.

From the point of view of the atrium, the cardiac cycle can be described as follows. After atrial depolarization (recognized from the P wave in the ECG) atrial sarcomeres contract (i.e., shorten). This event corresponds to late
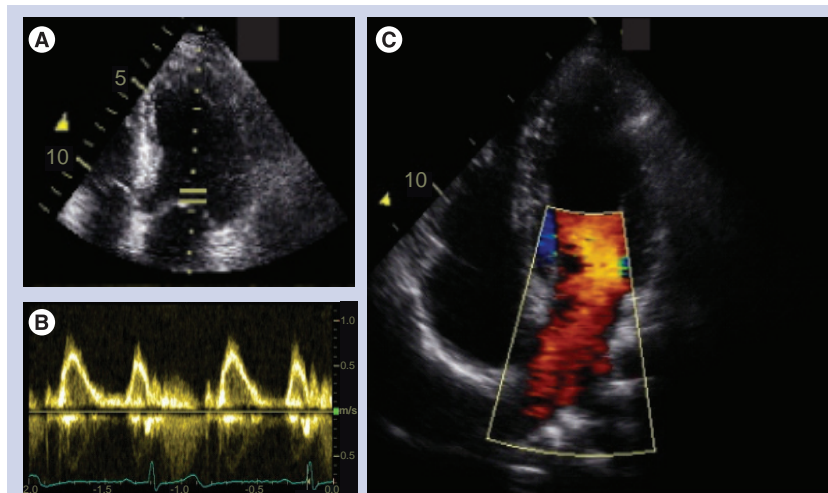
diastole of the ventricle. After mitral valve closure, during ventricular systole, the atrium fills and thus its volume increases and sarcomeres lengthen. This is the reservoir phase. Then, upon mitral valve opening, blood rapidly flows from the atrium to the ventricle and atrial volume decreases, sarcomeres shorten and the atrium serves as a conduit until the next depolarization wave arrives. This is the atrial conduit phase. Minimal changes of sarcomere length and atrial volume are observed during ventricular diastasis.

■ Myocardial deformation

In order to describe the way in which a myocardial segment deforms, the concepts of 'strain' and 'strain rate' as known in continuum mechanics were first applied to the heart in 1974 by Mirsky and Parmley [5]. Strain (denoted by the Greek letter 'ε') is a dimensionless parameter measuring the change in shape of an object relative to its original shape. In the case of a 1D object (i.e., an elastic chord), the only shape change is represented by lengthening/shortening. As such, its strain would be expressed mathematically as:

$$\varepsilon = \frac{L - L_0}{L_0}$$

where ε is the strain, L_0 is the initial length of the chord and L is the length after deformation (Figure 4). As strain is the change in length $(L - L_0)$ relative to the original length (L_0), it is a dimensionless quantity that is typically expressed as a percentage.

The rate at which the deformation takes place is simply the change in strain $(d\varepsilon)$ per unit of time (dt) and is referred to as the strain rate (SR):

$$SR = \frac{d\varepsilon}{dt}$$

SR is the ratio of a dimensionless unit (i.e., strain) to time and is thus expressed in units of 's^{-1}'.

The concept of strain and SR as explained for a 1D object above can be generalized. Indeed, as all 3D objects do, the heart deforms in three dimensions: along the radial axis (perpendicular to the epicardium, pointing out from the cavity), along the longitudinal axis (perpendicular to the radial axis, pointing towards the base) and along the circumferential axis (perpendicular to radial and longitudinal axes and directed anticlockwise around the classical echo short axis image) (Figure 5) [6]. One can thus talk about radial, longitudinal and circumferential strain (rate) in order to refer to the different deformation components of a 3D myocardial segment.
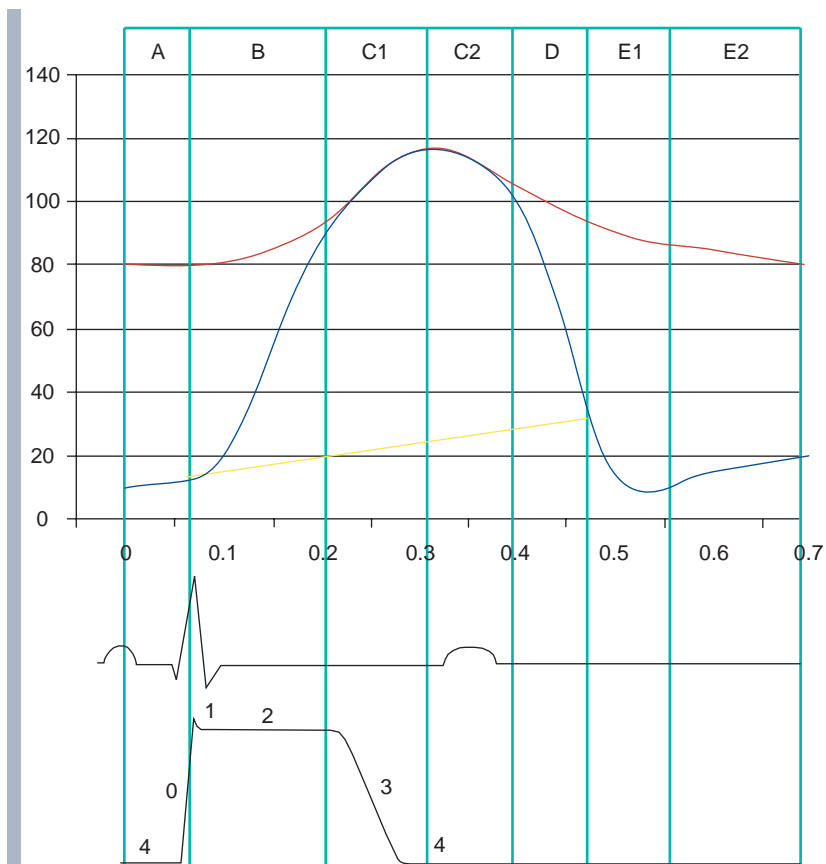

Figure 3. Schematic Wiggers diagram showing the aortic (red), left ventricular (blue) and left atrial (yellow) pressures over the cardiac cycle, together with the ECG.

In addition to the three deformation components described above (i.e., radial, longitudinal and circumferential strain), a myocardial segment will also show shear deformation (i.e., sliding of one border of the segment with respect to another one) (Figure 6). As such, the full characterization of the deformation of a myocardial segment, besides the three normal strain components, requires knowledge also on three shear strain components: circumferential–longitudinal shear strain,
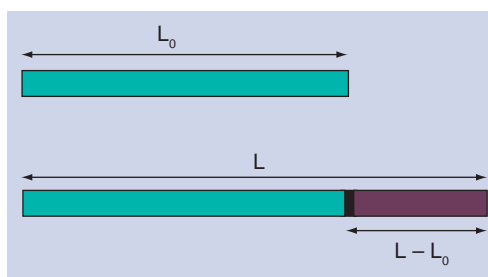
Figure 4. Amount of deformation of an elastic chord can be quantified by expressing the length change (L – L$_0$) relative to its original length (L$_0$). This quantity is defined as the 'strain' of the chord.
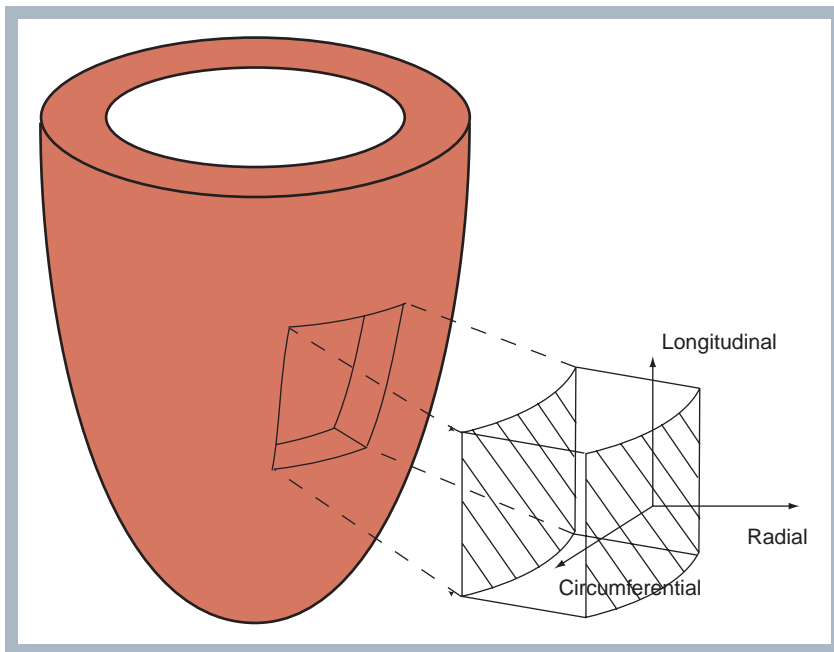
Figure 5. The deformation of a myocardial segment is expressed in terms of three physiologically relevant axes. The radial axis is perpendicular to the epicardium, the longitudinal axis is tangential to the pericardium and pointing from the apex of the ventricle to the base and the circumferential axis is tangential to the pericardium and orthogonal to the radial and longitudinal axis.

circumferential–radial and radial–longitudinal shear strains [7]. These shear strain components have been studied less extensively, although a few studies using new ultrasound methodologies have tried to look into this [8,9]. It should be noted that circumferential–longitudinal shear expresses the local contribution to global ventricular torsion. As such, the spatial integral of circumferential–longitudinal shear strain from base to apex is identical to global ventricular torsion.

As a result of the constant cyclic shortening and lengthening of the myocardial fibers, typical patterns of deformation throughout the cardiac cycle can be observed: during systole the ventricle undergoes longitudinal and circumferential shortening (negative strain) and radial thickening (positive strain), whereas during diastole it undergoes longitudinal and circumferential lengthening and radial thinning (Figure 7). All strain components show a gradient across the cardiac wall and typically increase from the subepicardial towards the subendocardial layer. This gradient is particularly strong for the circumferential strain component.

Similarly, longitudinal and circumferential shortening (negative strain) as well as radial thickening (positive strain) occurs in the atrial wall during atrial contraction. The atrial reservoir period is associated with longitudinal/circumferential lengthening (positive strain) and radial thinning (negative strain) (Figure 7).

Obviously, for a more complete description of the characteristics of the deformation of the heart not only strain, but also the SR has to be evaluated. During systole the shortening of the ventricular myocardium in the longitudinal and circumferential direction results in negative SR and the thickening in the radial direction results in positive (radial) SR. In diastole normally two SR peaks are present: one in the early and one in the late diastolic phase. Again longitudinal and circumferential SR are positive as the myocardium lengthens in these directions during diastole and radial SR is negative as the myocardium thins (Figure 7).

The atrial strain curves typically show the following SR peaks: SR peak during the atrial contraction period, two SR peaks during the atrial filling and one SR peak during early ventricular filling (Figure 7).

Myocardial deformation imaging

Myocardial strain and SR values can be obtained in a clinical setting using either Doppler myocardial imaging (DMI) [6,10] or speckle tracking [11,201] techniques. In this section, both approaches will be presented from a technical point of view and their respective strengths and weaknesses will be discussed.

■ Doppler myocardial imaging

Doppler myocardial imaging measures the velocity of the myocardium relative to the transducer in a similar way as the conventional Doppler systems. The system is set-up in such a way as to filter out high velocities from small reflective regions as these characteristics are typical for blood. As such, only the (relatively) slow velocities of the stronger reflecting regions (i.e., the myocardium) are retained.

During systole the base of the (normal) ventricle moves towards a relatively static apex. As a result, the velocity of the normal myocardium increases from the apex to the base. This velocity difference along the myocardial wall is referred to as a velocity gradient. Using a simple mathematical derivation, it can be proven that this velocity gradient per unit length is equal to the SR. Indeed, as defined above, strain (ε) can be written as: $\varepsilon = \Delta L/L_0$ (Figure 3). Using the definitions in Figure 8, this can be rewritten as: $\varepsilon = (D_2 - D_1)/L_0$ with D_1 and D_2 being the displacement of point 1 and 2, respectively. As SR is the change of strain with time, we can rewrite

this again as: $d\varepsilon/dt = (dD_2/dt - dD_1/dt)/L_0$. As the change of position with time (dD_1/dt) is nothing but the velocity of that point, this results in: $SR = (v_2 - v_1)/L_0$. In other words, the SR equals the spatial gradient in velocities.

The regional SR (i.e., rate of deformation) can thus be estimated by measuring the spatial gradient of the measured myocardial velocities [6]. By integrating the SR curve over time, the myocardial strain can be obtained. The latter is identical to deducing the distance a car has traveled from its origin given the speed of the car at every moment is known.

■ 2D speckle tracking

An alternative method to assess myocardial deformation is based on tracking specific grayscale patterns from one B-mode image to the next. Indeed, as the detailed microstructure of different myocardial tissue segments and their position relative to the transducer is not identical, each segment will show in the corresponding B-mode image as a unique grayscale pattern (which is referred to as 'speckle'). Tracking these grayscale patterns over time thus allows tracking of the motion of the underlying myocardial tissue. This process is schematically illustrated in **Figure 9**. In practice, a specific region (i.e., the 'kernel') is defined in one frame and sought for within a defined 2D area in the next frame. As such, the in-plane motion of the tissue segment can be tracked throughout the cardiac cycle.
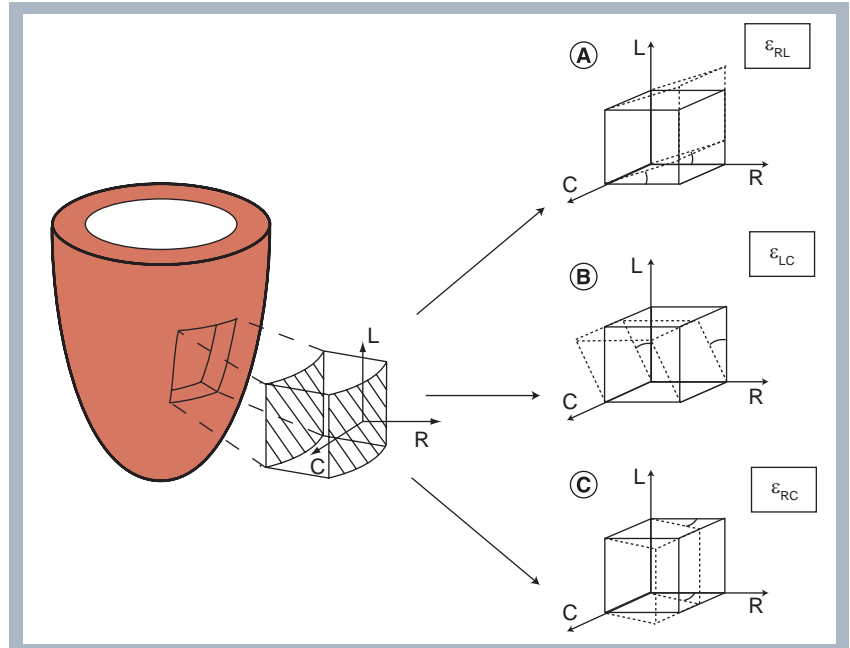
Figure 6. Shear strain components of the left ventricle. Shear strain refers to the sliding of one side of a small cube of myocardium with respect to the other side. The three shear strain components: ε_{RL} **(A)**, ε_{LC} **(B)** and ε_{RC} **(C)**, together with three normal strain components, completely determine the deformation of a myocardial segment.
ε_{LC}: Longitudinal–circumferential shear strain; ε_{RC}: Radial–circumferential shear strain; ε_{RL}: Radial–longitudinal shear strain; C: Circumferential; L: Longitudinal; R: Radial.

In practice, the speckle pattern does not repeat perfectly from one frame to the next, which can make the aforementioned process rather challenging.
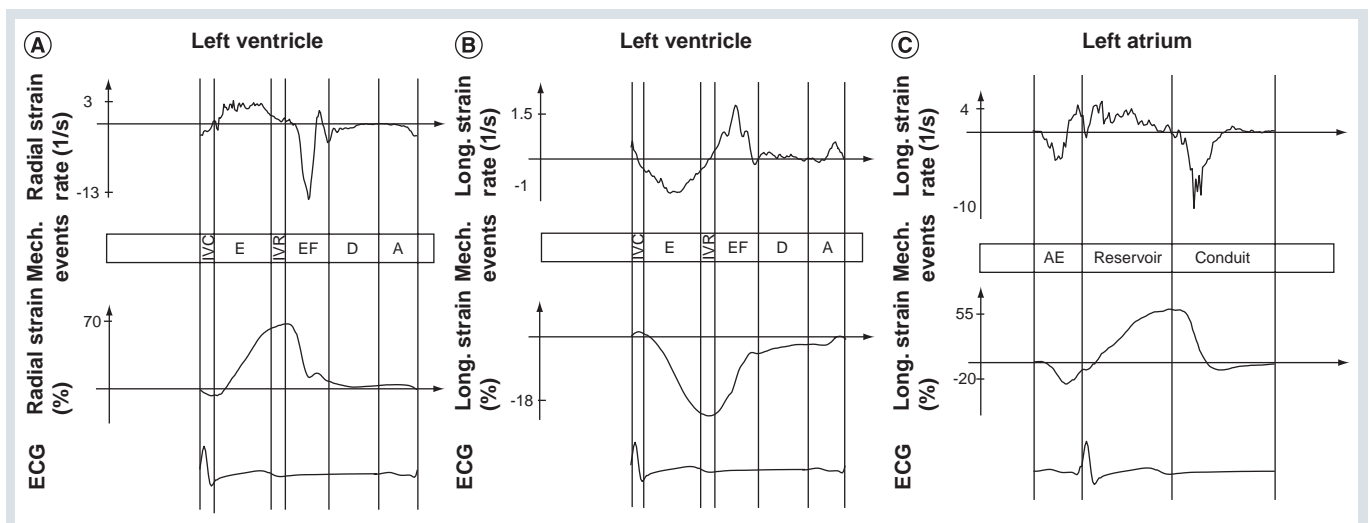
Figure 7. Normal strain rate and strain curves together with the ECG and timing of cardiac mechanical events measured in the left ventricle and atrium. (A) Strain rate (top) and strain (middle) curves measured in the left ventricle in the radial direction, **(B)** strain rate (top) and strain (middle) curves measured in the left ventricle in the longitudinal direction and **(C)** strain rate (top) and strain (middle) curves measured in the left atrium in the longitudinal direction. Vertical lines represent the timing of the cardiac mechanical events.
A: Atrial filling; AE: Active contraction; D: Diastasis; E: Ejection; EF: Early filling; IVC: Isovolumetric contraction; IVR: Isovolumetric relaxation.
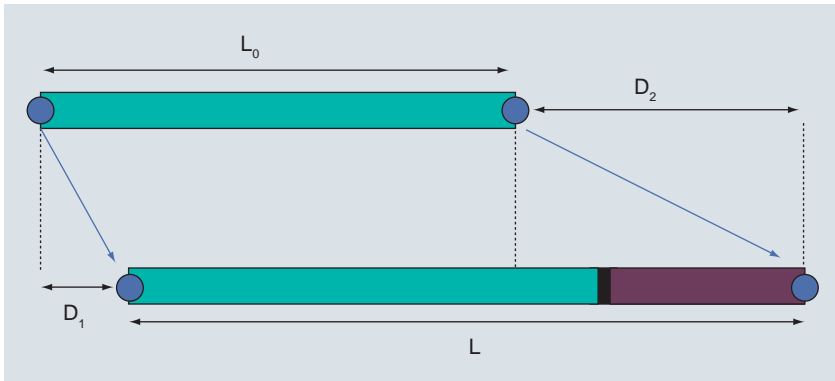
Figure 8. Definitions used to show that the myocardial velocity gradient equals the strain rate.
D_1: Displacement of the point 1; D_2: Displacement of the point 2; L: Length after deformation; L_0: Initial length.

When the positions of two kernels are known, their relative displacement per unit distance can be calculated, which equals the instantaneous strain of the tissue segment. Cumulating this instantaneous strain over all frame-pairs of a cardiac cycle results in the myocardial strain curves. SR can then be calculated as the temporal derivative of this curve.

■ **DMI versus 2D speckle tracking**
It might seem strange that strain and SR values derived from DMI and 2D speckle tracking correlate well but have different absolute values [11]. The reason for this discrepancy is that these two methods measure the same deformation of the heart in different ways, as will be discussed below. As such, both approaches have their specific advantages and disadvantages.

First, Doppler and speckle tracking intrinsically measure a different physical quantity. Doppler measures the instantaneous velocity of a point in one frame and can deduce the displacement of that point to the next frame by multiplying this velocity with the time period (dt) between both acquisitions. On the other hand, speckle tracking measures the displacement of a tissue segment from one frame to the next. From this displacement, the mean velocity over the time interval (dt) can be calculated by simple division. As long as acceleration of the tissue between both image frames is negligible, the difference between the instantaneous (Doppler) and the mean (speckle tracking) velocity will
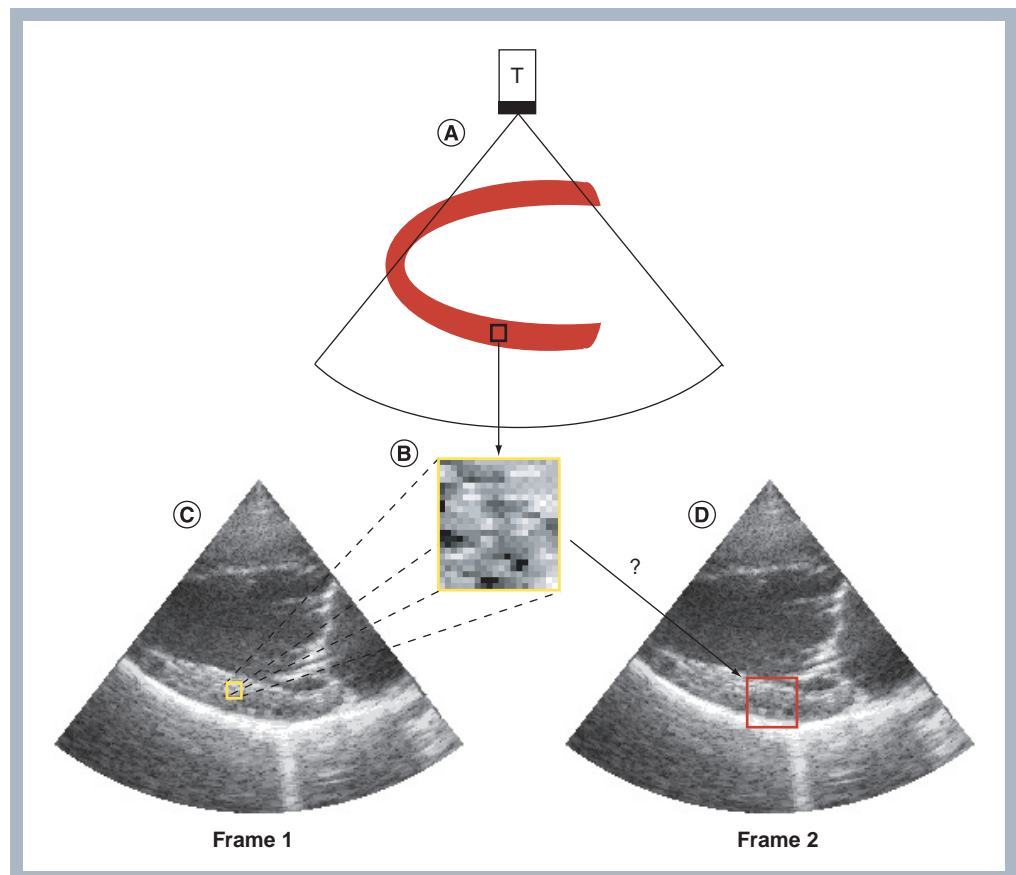
Figure 9. Schematic illustration of the principle of speckle tracking. A particular segment of myocardium **(A)** is represented in the ultrasound image by a grayscale pattern **(B)**. This pattern is unique and can be tracked from one frame to the next. Hereto, a kernel is defined (small region of gray values) in one frame **(C)** and sought for the in the next frame **(D)**.

be negligible as well. However, as soon as there is acceleration/deceleration one can expect to measure differences.

Second, the Doppler technique can only measure motion (and therefore deformation) in the direction of the ultrasound wave propagation (i.e., in the direction of the ultrasound image line). As such, the measured velocity/deformation amplitude will become dependent on the angle between the ultrasound line and the myocardial segment under investigation (Figure 10A). On the contrary, speckle tracking is angle independent as it tracks speckles in 2D within the ultrasound image and not only in the direction of the ultrasound line. It should be noted, however, that estimating the motion orthogonal to the image line remains intrinsically less accurate than measuring the motion along the image line. As such, speckle tracking also has a certain form of angle dependency [201].

Using apical imaging views, the Doppler approach can thus measure longitudinal strain and SR curves reliably in all left ventricular (LV) segments and in the free wall of the right ventricle (RV), as the ultrasound line can be well aligned with the longitudinal direction (Figure 10B). Moreover, it allows assessment of the longitudinal deformation characteristics in all atrial segments except for the atrial roof. Radial and circumferential strain (rate) can only be measured accurately in certain LV segments using a parasternal short or long axis view.

Speckle tracking on the other hand can give longitudinal and radial strain and SR curves in apical images as well as circumferential and radial strain (rate) in parasternal images (Figure 10C). As such, it allows assessment of all normal strain components in all LV segments.

Third, in order to allow for more reliable tracking, line density in the ultrasound image needs to be relatively high, with results in frame rates of typically 50–70 Hz. These relatively low frame rates limit the temporal resolution of the method, thereby making its application in conditions of high heart rates (i.e., during stress testing) impractical. DMI, on the other hand, offers a better temporal resolution as it typically works at much higher frame rates (>180 Hz). Resolving true motion/deformation characteristics of short-lived events during the cardiac cycle (e.g., ventricular untwist rate) might thus be more accurately assessed using the Doppler approach [12].

Finally, it should be noted that both methods are fairly sensitive to noise. As a consequence the data typically have to be filtered (i.e., spatially and temporally smoothed), which limits both spatial and temporal resolution. Moreover, it implies that the accuracy of the measurements of either method is strongly dependent on image quality. For this reason, images for DMI or speckle tracking should preferably be acquired during breath-hold as this avoids artifacts induced through respiratory motion. Similarly, care has to be taken to avoid reverberations in the ultrasound images as much as possible.

Whatever method used, a meaningful and reliable strain (rate) curve can only be obtained when the region of interest follows the same anatomical region throughout the cardiac cycle and avoids signals from the blood or pericardium [13]. For the Doppler approach, this tracking has to be done manually as no information is available on the motion orthogonal to the image line. Although semi-automatic tracking tools have been presented [14], processing these Doppler data sets therefore remains time consuming and labor intensive. For the speckle tracking approach, on the other hand, tracking of the region of interest can be done fully automatically, which speeds up analysis time tremendously. Mostly for this reason, speckle tracking has more potential as a method to be used in daily clinical practice.

◼ Validation

Every new imaging modality has to undergo validation before it can be introduced into clinical practice and before it can influence decision-making. Doppler-based and speckle-tracking-based myocardial deformation imaging were no exceptions. Both approaches have been validated in gel phantoms [15,16], in open-chest
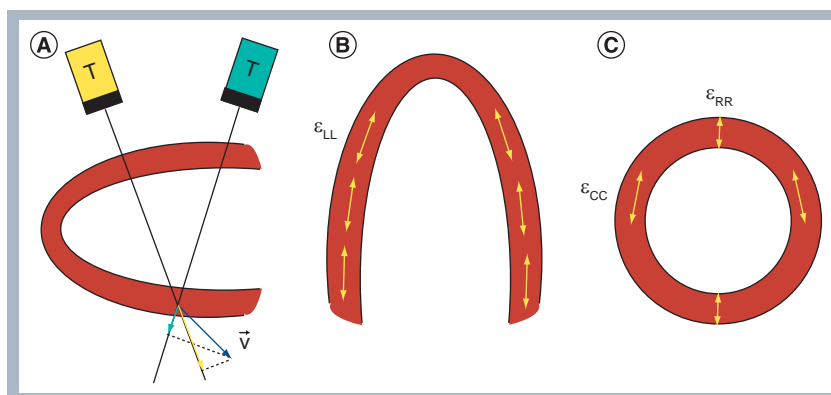
Figure 10. Doppler-based motion and strain estimation. Demonstrates an angle dependency, as this approach can only detect the motion/deformation along the ultrasound line **(A)**. As a consequence, this methodology can only be used to measure ε_{LL} (rate) in all left ventricular and right ventricular free wall segments **(B)**; ε_{RR} (rate) in the anteroseptal and posterior segments and ε_{CC} (rate) in the septal and lateral wall segments **(C)**.
ε_{CC}: Circumferential strain; ε_{LL}: Longitudinal strain; ε_{RR}: Radial strain; T: Transducer; V: Velocity vector.

animal models against sonomicrometry [16–21] and in human subjects against MRI with [22] or without [23] tagging. All these validation studies revealed that both of these methodologies allow sufficiently accurate and reproducible estimation of myocardial strain and SR *in vivo*. However, it has also been demonstrated that not only different methodologies (e.g., DMI or speckle tracking), but also different implementation by different vendors of ultrasound equipment provide different numerical strain and SR values [15]. This should always be taken into account when comparisons of deformation parameters are made. A direct comparison of the different implementations of the different vendors has, to date, not been performed.

■ Deformation parameters

Once the strain and SR curves have been measured throughout the cardiac cycle, different parameters can be extracted in order to characterize them. These parameters can be divided into those relating to timing and those relating to magnitude [13]. In order to characterize regional ventricular deformation, the magnitude parameters that are most often reported are the peak and/or end-systolic strain and the maximal systolic SR (Figure 11). Time-to-onset of deformation and time-to-onset of relaxation are typical

timing parameters, which can be used to evaluate the synchronicity of the ventricle. Postsystolic strain is an additional parameter, important for the recognition of ischemic segments, that combines magnitude with timing as it combines the deformation occurring after the end of the ejection period with the deformation occurring during the ejection period (Figure 11) [13].

Left ventricular twist is typically characterized by presenting the peak systolic twist and the peak diastolic untwist rate. Instead of peak systolic twist, peak systolic torsion is often used, which can be calculated by dividing peak systolic twist by the long axis dimension of the LV.

Although deformation imaging was originally introduced as a means to measure regional myocardial function, recently the average segmental lengthening/shortening of the LV (referred to as 'global' LV strain) has been proposed as an index of global cardiac function that could be more sensitive than conventional measurements of ejection fraction [24].

It should emphasized, however, that longitudinal, circumferential and radial strain are not interchangeable and might have different prognostic and diagnostic value in different conditions. Most of the studies so far have used longitudinal strain and SR. This choice was mainly based on practical issues. As already mentioned, DMI is capable of measuring longitudinal motion and deformation in all myocardial segments from well-aligned apical views, whereas circumferential and radial motion and deformation can be derived only in certain LV segments from parasternal views. As such, most DMI-based deformation imaging studies measured longitudinal strain. However, some studies have demonstrated that circumferential and/or radial strain might be more sensitive to detect abnormalities in certain pathologies or in certain applications [25–27]. With the introduction of the speckle tracking methodology, radial and/or circumferential strain can be assessed in all LV segments from the parasternal short axis images, although this is not commonly done as it remains more challenging to acquire appropriate data sets.

It is very important to note that none of the deformation parameters described above are a direct measure of myocardial contractility (i.e., contractile force). Indeed, all of these parameters depend not only on the contractile status of the muscle fibers, but also on the passive elastic properties of the tissue, on pre- and after-load [10,28,29]. It is known that strain and SR values increase with increasing preload and decrease with increasing afterload or ventricular
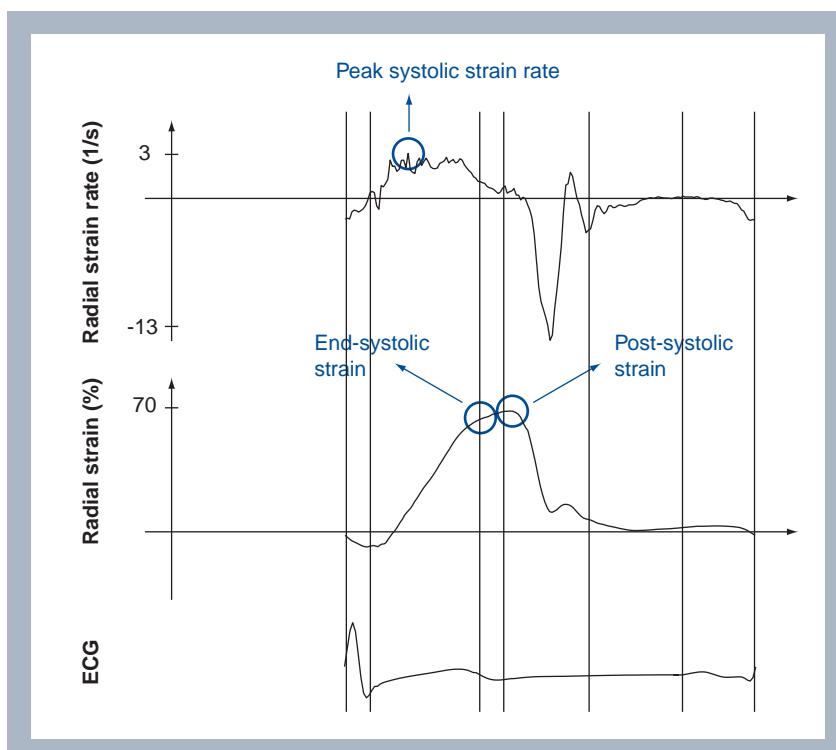

Figure 11. Parameters most often extracted to characterize the local strain and strain rate behavior.

size even without any changes in myocardial contractility [10,28–30]. In general, SR shows a good correlation with dP/dT_{max} and other invasive measures of contractility such as end-systolic elastance [28–31], but it is independent of heart rate [28–32]. On the other hand, myocardial strain seems to be more closely related to the changes in loading conditions of the ventricle [10].

Clinical applications

■ Normal values

For a parameter to be used as a classifier for disease in clinical practice its normal values should be known. Therefore, several studies have estimated the ranges of mean strain and SR values in the normal population [33–38]. They revealed that in healthy subjects mean LV longitudinal strain values, measured with tissue doppler imaging, range from -15 to -25% while mean radial strain values range from 50 to 70%. Longitudinal and radial SR values were reported to range from -1.0 to -1.4 s^{-1} and from 3.1 to 4.1 s^{-1}, respectively [33–36].

The studies, where strain imaging was performed with 2D techniques, revealed that peak LV longitudinal strain values range from -16 to -22% [37,38], whereas peak circumferential and radial strains range from -21 to -26% and from 37 to 39%, respectively [38].

Data regarding the effect of aging on strain and SR values are inconsistent. Some studies show that longitudinal systolic strain and SR values are independent of age [34,35], whereas other large general-population studies have demonstrated that both longitudinal and radial strain and SR independently decrease with age [36,37]. The data regarding gender differences in strain and SR values are also controversial. While in one of the big population studies radial strain (but not SR) was significantly higher in women and no gender differences in systolic longitudinal strain or SR were observed [36], in other studies longitudinal strain (but again not SR) was significantly higher in women [35,37]. To date, this issue remains unresolved.

It has also been shown that obese patients without overt heart disease exhibit significantly lower longitudinal and radial strain and SR values than lean subjects [36,39]. However, it is questionable whether obese patients can be considered as normal subjects as the alterations of LV deformation might be due to preclinical heart disease that cannot be detected with conventional methods.

Normal atrial strain and SR values are not so well defined. In different studies normal values of peak atrial strain range from -10 to -30% in the contractile period and from 12 to 85% in the filling period [40–42]. Peak atrial SR values ranged from -1 to -6.7 s^{-1} in the contractile period, from 1 to 8 s^{-1} in the filling period and from -1.8 to -11 s^{-1} in the conduit period [40–42].

The high range of atrial strain and SR values reported in these studies might of course be due to the different methodologies used. Generally, higher values were obtained when atrial deformation was assessed by the DMI approach [40]. However, atrial strain and SR values might also be biased if the membranous part of the atrial septum, atrial appendage or pulmonary vein inflow is not excluded from the calculations.

The variability of atrial deformation in the general population has also been studied, although not extensively. It has been shown that peak atrial strain of the ventricular filling period decreases with increasing age and increasing BMI. Negative correlation has also been observed between age and peak atrial contraction and conduit period SR, as well as between BMI and peak atrial filling SR [41].

Finally, it should be emphasized once again that normal values are both methodology (i.e., Doppler vs speckle tracking) and technology (i.e., hardware/software and therefore vendor) specific. Nevertheless, general trends of strain (rate) dependency on demographic variables are less likely to be influenced by this.

■ Ischemic heart disease

Numerous clinical and experimental studies have been performed to investigate the applications of SR imaging in the setting of ischemic heart disease. It has been shown that in acutely or chronically ischemic myocardium the peak systolic strain and SR are reduced, while the amount of postsystolic deformation increases [43–48]. Comparison with MRI has shown that both strain and SR are significantly lower in the segments with transmural infarction than in the ones where necrosis was limited to the subendocardial layer only [46–48].

The application of SR imaging in assessing myocardial viability has been extensively studied in animal models as well as in humans [48–55]. Systolic strain, SR and postsystolic strain respond differently to the dobutamine infusion in different ischemic substrates (Table 1). As this response depends on the regional perfusion, this stress test helps distinguishing stunned myocardial segments from ischemic ones and can help to estimate the transmurality of myocardial infarction [28,30,49].

Interestingly, dipyridamole infusion, which is known to reduce regional coronary flow, did not induce the same changes of regional

Table 1. The response of different ischemic substrates to a dobutamine challenge.

Ischemic substrate	Parameter	Rest	Low dose dobutamine	High dose dobutamine
Normal myocardium	SR_{peak}	N	↑	↑
	ε_{ES}	N	↑	↓
	ε_{PS}	N	→	→
Stunned myocardium	SR_{peak}	↓	↑	↑
	ε_{ES}	↓	↑	↓
	ε_{PS}	↑	↓	→
Acute ischemia	SR_{peak}	↓	↓	↓
	ε_{ES}	↓	↓	↓
	ε_{PS}	↑	↑	↑
Subendocardial infarction	SR_{peak}	↓	↑	↓
	ε_{ES}	↓	→	→
	ε_{PS}	↑	→	↑
Transmural infarction	SR_{peak}	↓	→	→
	ε_{ES}	↓↓	→	→
	ε_{PS}	↑	→	→

Changes are expressed relative to normal rest conditions. For low dose and high dose dobutamine challenges, these changes are with respect to the rest and low dose conditions of the same ischemic substrate, respectively.
↓: Decreased; ↑: Increased; →: No change; ε_{ES}: End-systolic strain; ε_{PS}: Postsystolic strain; N: Normal; SR_{peak}: Peak systolic strain rate.

deformation in normal, stunned or infarcted myocardium [55]. This might be due to the different pharmacodynamics of dipyridamole and dobutamine.

From these studies it is clear that SR imaging (potentially combined with a SR study during stress testing) can contribute to the follow-up of patients with ischemic heart disease or to the assessment of successful revascularization procedures. Interestingly, there is evidence that SR imaging could help to select patients with severe LV dilation due to ischemic cardiomyopathy for surgical ventricular restoration [56] or to monitor the effect of new therapeutic strategies [57].

■ Myocardial diseases

Numerous studies have elucidated the utility of SR imaging in the differential diagnosis of myocardial disease as well as in their detection of subclinical disease.

Although in the presence of hypertrophic cardiomyopathy global systolic function is usually normal, the introduction of myocardial deformation imaging revealed that systolic deformation is already significantly reduced in these patients [58–61].

The data from the study comparing patients with hypertensive LV hypertrophy with patients in whom LV hypertrophy was due to excessive strength training show that SR imaging may help to distinguish these two types of hypertrophy [59]. In this study, hypertensive patients exhibited postsystolic strain and significantly reduced peak systolic strain, peak systolic SR and early diastolic SR when compared with athletes who had normal deformation patterns [59]. It has been shown that a DMI-derived longitudinal systolic strain value below -10.6% is highly sensitive and specific for the detection of hypertrophic cardiomyopathy [60]. However, a study comparing myocardial deformation patterns in children with LV hypertrophy of various etiologies revealed no clear differences in any of these parameters between the groups, although they all were altered when compared with normal controls [61]. This would suggest that the myocardial deformation pattern is more influenced by the hypertrophy itself and less by the underlying cause.

The alterations of deformation are probably related to the presence of myocardial fibrosis, which would also explain why the athlete's heart deforms normally. Recently, it has been documented that in patients with hypertensive heart disease longitudinal LV and RV strain correlated independently with the circulating procollagen type III aminoterminal propeptide [62], showing that alteration of cardiac longitudinal function might be related to increased collagen III synthesis and increased myocardial fibrosis. Another study comparing deformation imaging patterns with late enhancement detected on MRI suggested that SR imaging is capable of detecting myocardial segments with nonischemic fibrosis, as these segments typically exhibit 'a double peak sign' (two SR peaks) [63].

Finally, myocardial deformation imaging may help to reveal subclinical myocardial involvement in noncardiac diseases such as amyloidosis, diabetic heart disease, β-thalassemia, Friedreich's ataxia or Duchenne muscular dystrophy [64–69]. It has been shown that decreasing radial and longitudinal systolic ε and SR enable the early detection of cardiotoxicity of anthracyclines [70–72].

■ Valvular heart disease

Assessment of global LV function in the setting of valvular heart disease is very important to choose the right timing for surgical intervention. Unfortunately, the information obtained by conventional echocardiography is not always sufficient to make a proper clinical decision. That is where myocardial deformation imaging might play a role.

As valvular disease progresses, myocardial deformation patterns change even before symptoms develop and before LV dysfunction can be

revealed by conventional methods. It has been reported that radial and longitudinal peak systolic SR were both decreased in patients with moderate and severe aortic regurgitation [73] as well as in patients with isolated mitral valve regurgitation [74,75]. In both of these groups of patients, deformation parameters correlated inversely with LV end-diastolic and end-systolic volumes [73,74]. Therefore, SR imaging might be useful in detecting subclinical deterioration of LV function and irreversible myocardial damage in asymptomatic patients with valvular insufficiencies [75]. It has been suggested that subclinical myocardial dysfunction revealed by SR imaging might help to decide the timing for surgical intervention [75].

In patients with aortic stenosis, peak systolic and end-systolic strain are reduced and correlate with aortic valve area and stroke volume [76]. After successful intervention these parameters are expected to improve [77,78].

■ RV function

In clinical routine RV function is usually evaluated qualitatively by assessing the RV free wall motion visually or by measuring tricuspid annular movement during the systole (i.e., tricuspid annular plane systolic excursion). Techniques based on volume or area changes that are used for the assessment of LV function are not easily applicable for the RV because of its complex geometry.

The evaluation of RV function with SR imaging is therefore promising, particularly because it is not influenced by overall heart motion. Although it remains challenging, SR imaging appears to be useful in the evaluation of RV function in pulmonary hypertension and arrythmogenic RV dysplasia [79–82]. It has been shown that patients with chronic pulmonary hypertension have significantly lower RV systolic strain and SR values than normal controls [79]. In the same study, RV apical strain also correlated with invasively measured mean pulmonary artery pressure and pulmonary vascular resistance. Moreover, in patients with chronic thrombembolic pulmonary hypertension, RV deformation patterns improve after a successful pulmonary endarterectomy [81].

■ Diastolic dysfunction

Currently, diastolic function is assessed by the analysis of the transmitral flow pattern and diastolic myocardial velocities. The ratio of early mitral inflow velocity to early diastolic mitral annular velocity (E/E') is known to correlate with relaxation abnormalities [83] and to reflect LV filling pressures [84]. As E reflects the pressure gradient between left atrium and LV and

E' reflects global LV volume change during the early diastole, the E/E' ratio provides information on how much volume enters the ventricle for a given left atrium–LV pressure gradient. As such, it can be inaccurate in situations where E' does not properly reflect global volume changes (e.g., in LV dilatation, large infarctions, primary mitral regurgitation or stenosis) [30].

Clearly, a parameter directly showing the stiffness of myocardium would be of great value in diastology. Such a parameter could be the diastolic strain and SR [13]. However, although some studies have used strain imaging for the evaluation of diastolic function [85,86], its value in this setting still remains unclear and needs further investigation.

Ventricular untwisting is known to primarily take place during the isovolumic relaxation phase. As such, measuring ventricular untwist rate is intrinsically independent of left atrial pressure and has been proposed as a good noninvasive parameter to assess LV diastolic function [87]. By combining the analysis of short axis images acquired at different levels in the LV both DMI and speckle tracking methodologies have been tested and correlated against invasive measures of diastolic function [12,88].

■ Atrial function

Atrial contraction is an important contributor to LV filling and, as a consequence, to cardiac output. In echocardiography, left atrial function is typically assessed by measuring its dimensions and volume, by the presence of an A wave on the transmitral pulsed wave Doppler pattern and by the presence of an atrial reversal wave on the pulsed wave Doppler signal recorded at the pulmonary vein inflow. However, these parameters are not always informative enough and myocardial deformation analysis could provide a more extensive evaluation of atrial function.

It has been shown recently that elevated LV end-diastolic pressure inversely correlates with left atrial filling strain [89] and that 89% of patients with atrial filling strain values below 30% had an elevated LV end-diastolic pressure (>16 mmHg). Atrial deformation is also altered in patients with hypertensive heart disease and allows subclinical detection of atrial dysfunction in these patients [90].

Moreover, evaluation of atrial deformation might be of interest in the setting of atrial fibrillation, which is the most frequent arrhythmic disorder nowadays, with very high recurrence rates after successful cardioversion. The value of atrial strain and SR in predicting the maintenance of

the sinus rhythm in these patients has already been explored in several studies [91,92]. These studies have shown that before cardioversion, patients in whom later sinus rhythm is maintained have higher atrial filling strain and SR values [91,92]. Similar results were obtained in another study where atrial SR imaging has been implemented for the prediction of maintenance of sinus rhythm after catheter ablation of atrial fibrillation [93]. The same study also showed that after catheter ablation patients who suffered from persistent atrial fibrillation had lower atrial filling strain and SR values when compared with patients with paroxysmal atrial fibrillation. A gradual increase in strain and SR values was observed in patients in whom sinus rhythm was maintained, but not in those with recurrent atrial fibrillation.

■ Heart failure

Heart failure is one of the biggest burdens of the aging western community. It is a very complex clinical syndrome with high mortality and morbidity rates. Echocardiography is an irreplaceable clinical tool in the follow-up of these patients and SR imaging has several potential clinical applications in this setting as well.

Global longitudinal and circumferential strains derived from 2D speckle tracking appear to be powerful predictors of cardiac events, including deaths and hospitalizations, in patients with heart failure [27]. An especially strong and independent prognosticator in this study was global circumferential strain, which was also superior to global longitudinal strain and LV ejection fraction.

Cardiac resynchronization therapy is now widely used for the treatment of patients with heart failure due to dilated cardiomyopathy and left bundle branch block. In these patients abnormal conduction leads to the delayed activation and contraction of the lateral LV wall as a result of suboptimal pump function. In properly selected patients cardiac resynchronization therapy corrects this delay and significantly reduces heart failure symptoms. ECG signs of left bundle branch block, showing only the electrical activation of the heart, do not always correlate well with the true ventricular mechanics [94]. Therefore, echocardiography and especially myocardial velocity and deformation imaging seemed to be a valuable tool for the detection of mechanical intra- or interventricular dyssynchrony. Numerous studies have investigated dyssynchrony parameters derived from myocardial velocity and deformation data (e.g., time delay between peak systolic SRs/peak systolic velocities of opposite LV walls). However, to date, the data regarding the predictive value of

these parameters in selecting patients for cardiac resynchronization therapy are very contradictory [94–99]. The multicenter clinical PROSPECT trial concluded that because of low sensitivity and specificity no single echocardiographic parameter can be recommended for the assessment of ventricular dyssynchrony and for patient selection for cardiac resynchronization therapy (CRT) [100]. Apparently, these results were influenced by high levels of both inter- and intra-observer variability, as reported in the study, and the predictive value of the echocardiographic parameters tested could potentially be increased by better expertise and training. Moreover, in the PROSPECT trial, dyssynchrony was estimated from longitudinal motion and deformation, which might not be so sensitive in predicting response to CRT as circumferential or radial deformation [25,26].

Quite recently, two other echocardiographic parameters that may help to predict CRT response have been introduced. First, the 'septal flash' or early septal thickening/thinning within the isovolumic contraction period [101]. It results from the early activation of the intraventricular septum in the presence of left bundle branch block and can be visualized on both parasternal short and long axis images using grayscale or tissue Doppler color M-mode. After successful CRT the 'septal flash' has been shown to resolve [101]. Another novel parameter quantifying the same phenomenon in a different manner is the longitudinal rotation alternatively referred to as apical transverse motion that can be calculated from longitudinal color tissue doppler imaging data [102,103].

In patients with LV-assist devices, myocardial deformation imaging appeared to be useful in the evaluation of myocardial recovery during mechanical unloading and in selecting patients for the assist device explantation [56,104]. However, determining the role of deformation imaging in this setting is challenging, as a very high level of expertise of both the echocardiographer and surgeon is required in order to perform these interventions and select the proper patients for it.

■ Cardiac allograph dysfunction

It has clearly been shown that in heart transplant patients with relevant cardiac allograph vasculopathy, myocardial longitudinal and radial peak systolic ε and SR are markedly reduced and correlate well with histological and angiographical findings [105–107]. In combination with dobutamine stress echocardiography, SR imaging might reveal cardiac allograph vasculopathy even when no significant stenoses can be detected during coronary angiography [107]. Acute heart transplant

rejections can also be detected even in asymptomatic patients by a sudden drop of longitudinal or radial SR [108]. Thus, myocardial deformation imaging offers the possibility to detect cardiac allograph vasculopathy and acute allograph rejection and to reduce the need and frequency of invasive diagnostic procedures routinely performed for the heart transplant patients.

Conclusion
Strain and SR imaging have become a valuable clinical tool as they allow noninvasive quantification of the way in which the cardiac muscle deforms during the cardiac cycle at a segmental level. Until recently, this was only possible through invasive measures that mostly limited these studies to the experimental setting. Strain and SR imaging is highly useful in settings where subtle changes in myocardial function have to be detected and where conventional echocardiography reaches its limits, for example in detecting heart disease at its preclinical stage or in therapy monitoring. Moreover, deformation imaging methods might help to reveal the (patho) physiological processes underlying some of the heart diseases.

Although deformation imaging was originally introduced for the assessment of regional myocardial function, recent studies have shown that this methodology can provide an elegant tool to quantify global LV function with better prognostic value than conventional measurements such as ejection fraction.

Of course, in order to use this new modality adequately, a critical attitude and common sense in combination with a good knowledge of cardiac anatomy and pathophysiology remain indispensable. In addition, it is important to be familiar with the principles and limitations of the techniques used, as they will influence the obtained deformation curves and the extracted values.

Finally, it should be recognized that in spite of all the possibilities offered by SR imaging and in spite of all the elegant and promising studies presented in the literature, these techniques are still not fully integrated into routine clinical practice. The main reasons for this are the long off-line analysis time (although this has improved significantly in recent years), high interobserver variability (although this is comparable to currently used methodologies) and the lack of normal reference values. In addition, some of the concepts require a good understanding of cardiac mechanics and appear to be very mathematical and complex to some operators. Luckily, further technological developments will solve some of

these concerns by bringing semiautomatic segmentation software and improved tracking quality in more challenging conditions. This should make SR imaging even more user friendly and less observer dependent. Moreover, large population studies are being conducted to derive the normal values of deformation parameters, so as to test their real prognostic value in different pathologic conditions.

Future perspective
With the introduction of new matrix array transducer technology, volumetric ultrasound imaging has become more readily available. As a result, several methodologies have recently been developed allowing 3D strain estimation [109,110]. Some small-scale feasibility studies using these methodologies have been presented [111,112], but a thorough clinical evaluation of these 3D methods remains to be carried out. Theoretically, 3D methods have some advantages to offer. Indeed, these approaches can measure all strain components in all ventricular segments from a single acquisition. In addition, they can facilitate the assessment of LV twist mechanics, as several short axis images can be more easily aligned parallel. Finally, the 3D methodologies can speed up analysis time compared with the 2D speckle tracking or DMI methods [112]. On the other hand, these 3D strain methodologies require very high-quality volumetric data sets, which is challenging in clinical practice where shadows and drop-outs are often present. In addition, the volumetric data come at the expense of temporal resolution, which may limit its applicability to some clinical conditions (i.e., stress testing).

For the future, we can expect that myocardial deformation imaging will become a 3D technique that allows the characterization of segmental wall deformation at high spatial and temporal resolution in a reproducible manner. As such, these new imaging modalities are expected to find their way into clinical routine practice and will help improve diagnosis and therapy of individual patients.

Executive summary

- Quantification of regional myocardial function has evolved from a qualitative visual reading to a quantitative analysis of regional wall deformation characteristics.
- Two different approaches have been developed and clinically evaluated:
  - Doppler-based measurements: strain and strain rate are derived from the Doppler velocity data set as the (temporal integral of the) spatial velocity gradient. The major disadvantage of this approach is that it is angle dependent.
  - Speckle tracking-based measurements: strain and strain rate are derived from the speckle tracking frame-to-frame displacements. The major disadvantage of this approach is that for most implementations the spatial and temporal resolution remains limited.
- Both methodologies have been validated in gel phantoms, in animals against sonomicrometry and in humans against MRI (tagging).
- Both methodologies have been applied in a multitude of clinically relevant settings and have shown their benefits over the conventional approach.
- Future methodologies will improve the spatial and temporal resolution of the strain (rate) data set, as well as speed up the postprocessing.

Bibliography

Papers of special note have been highlighted as:
- of interest

1 Hoffmann R, Lethen H, Marwick T *et al.*: Analysis of interinstitutional observer agreement in interpretation of dobutamine stress echocardiograms. *J. Am. Coll. Cardiol.* 27(2), 330–336 (1996).

2 Picano E, Lattanzi F, Orlandini A *et al.*: Stress echocardiography and the human factor: the importance of being expert. *J. Am. Coll. Cardiol.* 17, 666–669 (1991).

3 Sutherland GR, Stewart MJ, Groundstroem WE *et al.*: Color doppler myocardial imaging: a new technique for the assessment of myocardial function. *J. Am. Soc. Echocardio.* 7, 441–458 (1994).

4 Tsutsui H, Uematsu M, Shimizu H *et al.*: Comparative usefulness of myocardial velocity gradient in detecting ischemic myocardium by a dobutamine challenge. *J. Am. Coll. Cardiol.* 31, 89–93 (1998).

5 Mirsky I, Parmley WW: Assesment of passive elastic stiffness for isolated heart muscle and the intact heart. *Circ. Res.* 33(2), 233–243 (1973)

- **Gives a thorough explanation of cardiac mechanics including the fundamental concepts of myocardial stress and strain.**

6 D'hooge J, Heimdal A, Jamal F *et al.*: Regional strain and strain rate measurements by cardiac ultrasound: principles, implementation and limitations *Eur. J. Echocardiogr.* 1, 154–170 (2000).

- **Reviews the technical principles behind Doppler-based strain estimation and discusses some practical aspects when implementing this methodology in practice.**

7 Bogaert J, Rademakers FE: Regional nonuniformity of normal adult human left ventricle. *Am. J. Physiol. Heart. Circ. Physiol.* 280, H610–H620 (2001).

8 Separovic Hanzevacki J, Claus P, Herbots L *et al.*: Assessment of circumferential-radial shear strains in normal and ischemic myocardium based on ultrasonic strain/strain rate imaging. *Eur. Heart J.* 4, 521 (2002).

9 Barbosa D, Claus P, Choi HF, Hristova K, Loeckx D, D'hooge J: An *in vivo* study on the difference between principal and cardiac strains. *IEEE Proceedings of the International Ultrasonics Symposium* 1411–1414 (2009).

10 Sutherland GR, Hatle L, Claus P, D'hooge J, Bijnens BH: *Doppler Myocardial Imaging-A Textbook.* BSWK, Hasselt, Belgium (2006).

- **Gives a very thorough explanation of the principles of Doppler-based strain estimation together with a state-of-the-art review of current clinical applications.**

11 Perk G, Tunick PA, Kronzon I: Non Doppler two dimensional strain imaging by echocardiography – from technical considerations to clinical applications. *J. Am. Soc. Echocardiogr.* 20, 234–243 (2007).

- **Reviews some approaches used to perform 2D motion estimation based on speckle tracking.**

12 Ferferieva V, Claus P, Vermeulen K *et al.*: Echocardiographic assessment of left ventricular untwist rate: comparison of tissue Doppler and speckle tracking methodologies. *Eur. J. Echocardiogr.* 10(5), 683–690 (2009).

13 Marwick TH: Measurement of strain and strain rate by echocardiograhy. ready for prime time? *J. Am. Coll. Cardiol.* 47, 1313–1327 (2006).

14 Claus P, D'hooge J, Langeland T, Bijnens B, Sutherland GR: SPEQLE (software package for echocardiographic quantification leuven): an integrated approach to ultrasound-based cardiac deformation quantification. *Comput. Cardiol.* 29, 69–72 (2002).

15 Kjaergaard J, Korinek J, Belohlavek M, Oh JK, Sogaard P, Hassager C: Accuracy, reproducibility, and comparability of Doppler tissue imaging by two high-end ultrasound systems. *J. Am. Soc. Echocardiogr.* 19(3), 322–328 (2006).

16 Korinek J, Wang J, Sengupta PP *et al.*: Two-dimensional strain – a Doppler-independent ultrasound method for quantitation of regional deformation: validation *in vitro* and *in vivo*. *J. Am. Soc. Echocardiogr.* 18(12), 1247–1253 (2005).

17 Edvardsen T, Urheim S, Skulstad H, Steine K, Ihlen H, Smiseth OA: Quantification of left ventricular systolic function by tissue Doppler echocardiography: added value of measuring pre- and postejection velocities in ischemic myocardium. *Circulation* 105(17), 2071–2077 (2002).

18 Langeland S, Wouters PF, Claus P *et al.*: Experimental assessment of a new research tool for the estimation of two-dimensional myocardial strain. *Ultrasound Med. Biol.* 32(10), 1509–1513 (2006).

19 Pirat B, Khoury DS, Hartley CJ *et al.*: A novel feature-tracking echocardiographic method for the quantitation of regional myocardial function: validation in an animal model of ischemia-reperfusion. *J. Am. Coll. Cardiol.* 51(6), 651–659 (2008).

20 Reant P, Labrousse L, Lafitte S *et al.*: Experimental validation of circumferential, longitudinal, and radial 2-dimensional strain during dobutamine stress echocardiography in ischemic conditions. *J. Am. Coll. Cardiol.* 51(2), 149–157 (2008).

21 Helle-Valle T, Crosby J, Edvardsen T *et al.*: New noninvasive method for assessment of left ventricular rotation: speckle tracking echocardiography *Circulation* 112, 3149–3156 (2005).

22 Amundsen BH, Helle-Valle T, Edvardsen T *et al.*: Noninvasive myocardial strain measurement by speckle tracking echocardiography: validation against sonomicrometry and tagged magnetic resonance imaging. *J. Am. Coll. Cardiol.* 47(4), 789–793 (2006).

23 Herbots L, Maes F, D'hooge J *et al.*: Quantifying myocardial deformation throughout the cardiac cycle: a comparison of

ultrasound strain rate, grey-scale M-mode and magnetic resonance imaging. *Ultrasound Med. Biol.* 30(5), 591–598 (2004).

24   Stanton T, Leano R, Marwick TH: Prediction of all-cause mortality from global longitudinal speckle strain: comparison with ejection fraction and wall motion scoring. *Circ. Cardiovasc. Imaging* 2, 356–364 (2009).

25   Helm RH, Leclercq C, Faris OP *et al.*: Cardiac dyssynchrony analysis using circumferential versus longitudinal strain. implications for assessing cardiac resynchronization. *Circulation* 111, 2760–2767 (2005).

26   Delgado V, Ypenburg C, van Bommel RJ *et al.*: Assessment of left ventricular dyssynchrony by speckle tracking strain imaging comparison between longitudinal, circumferential and radial strain in cardiac resynchronization therapy. *J. Am. Coll. Cardiol.* 51(20), 1944–1952 (2008).

27   Cho GY, Marwick TH, Kim HS, Kim MK, Hong KS, Oh DJ: Global 2-dimensional strain as a new prognosticator in patients with heart failure. *J. Am. Coll. Cardiol.* 54(7), 618–624 (2009).

28   Weidemann F, Jamal F, Sutherland GR *et al.*: Myocardial function defined by strain rate and strain during alterations in inotropic states and heart rate. *Am. J. Physiol. Heart Circ. Physiol.* 283, H792–H799 (2002).

29   Rosner A, Bijnens B, How OJ *et al.*: Left ventricular size determines tissue Doppler-derives longitudinal strain and strain rate. *Eur. J. Echocardiogr.* 10(2), 271–227 (2009).

30   Bijnens BH, Cikes M, Claus P, Sutherland GR: Velocity and deformation imaging for the assessment of myocardial dysfunction *Eur. J. Echocardiogr.* 10, 216–226 (2009).

31   Derumeaux G, Mulder P, Richard V *et al.*: Tissue Doppler imaging differentiates physiological from pathological pressure-overload left ventricular hypertrophy in rats. *Circulation* 105, 1602–1608 (2002).

32   Weytjens C, D'hooge J, Droogmans S *et al.*: Influence of heart rate reduction on Doppler myocardial imaging parameters in a small animal model. *Ultrasound Med. Biol.* 35(1), 30–35 (2009).

33   Kowalski M, Kukulski T, Jamal F *et al.*: Can natural strain and strain rate quantify regional myocardial deformation? A study in healthy subjects. *Ultrasound Med. Biol.* 27, 1087–1097 (2001).

34   Sun JP, Popovic ZB, Greenberg NL *et al.*: Noninvasive quantification of regional myocardial function using Doppler-derived velocity, displacement, strain rate, and strain in healthy volunteers: effects of aging. *J. Am. Soc. Echocardiogr.* 17, 132–138 (2004).

35   Herbots L: Description of deformation values in healthy volunteers and the influence of BMI, age and gender. In: *Quantification of Regional Myocardial Deformation: Normal Characteristics and Clinical Use in Ischaemic Heart Disease.* Leuven University Press, Leuven, Belgium, 45–72 (2006).

36   Kuznetsova T, Herbots L, Richart T *et al.*: Left ventricular strain and strain rate in a general population. *Eur. Heart J.* 29, 2014–2023 (2008).

37   Marwick TH, Leano RL, Brown J *et al.*: Myocardial strain measurement with 2-dimensional speckle-tracking echocardiography: definition of normal range. *JACC Cardiovasc. Imaging* 2(1), 80–84 (2009).

38   Hurlburt HM, Aurigemma GP, Hill JC *et al.*: Direct ultrasound measurement of longitudinal, circumferential, and radial strain using 2-dimensional strain imaging in normal adults. *Echocardiography* 24(7), 723–731 (2007).

39   Wong CY, O'Moore-Sullivan T, Leano R, Byrne N, Beller E, Marwick TH: Alterations of left ventricular myocardial characteristics associated with obesity. *Circulation* 110, 3081–3087 (2004).

40   Sirbu C, Herbots L, D'hooge J *et al.*: Feasibility of strain and strain rate imaging for the assessment of regional left atrial deformation: a study in normal subjects. *Eur. J. Echocardiogr.* 7, 199–208 (2006).

41   Saraiva RM, Demirkol S, Buakhamsri A *et al.*: Left atrial strain measured by two dimensional speckle-tracking represents a new tool to evaluate left atrial function. *J. Am. Soc. Echocardiogr.* 23, 172–180 (2010).

42   Pinton RV, Moreno CA, Baxter CM, Lee KS, Tsang SM, Appleton CP: Two-dimensional speckle-tracking echocardiography of the left atrium: feasibility and regional contraction and relaxation differences in normal subjects. *J. Am. Soc. Echocardiogr.* 22, 299–305 (2009).

43   Voigt JU, Arnold MF, Karlsson M *et al.*: Assessment of regional longitudinal myocardial strain rate derived from Doppler myocardial imaging indexes in normal and infarcted myocardium. *J. Am. Soc. Echocardiogr.* 13(6), 588–598 (2000).

44   Jamal F, Kukulski T, Sutherland GR *et al.*: Can changes in systolic longitudinal deformation quantify regional myocardial function after an acute infarction? An ultrasonic strain rate and strain study. *J. Am. Soc. Echocardiogr.* 15(7), 723–730 (2002).

45   Abraham TP, Nishimura RA, Holmes DR Jr *et al.*: Strain rate imaging for assessment of regional myocardial function: results from a clinical model of septal ablation. *Circulation* 105(12), 1403–1406 (2002).

46   Jurcut R, Pappas CJ, Masci PG *et al.*: Detection of regional myocardial dysfunction in patients with acute myocardial infarction using velocity vector imaging. *J. Am. Soc. Echocardiogr.* 21(8), 879–886 (2008).

47   Weidemann F, Wacker C, Rauch A *et al.*: Sequential changes of myocardial function during acute myocardial infarction, in the early and chronic phase after coronary intervention described by ultrasonic strain rate imaging. *J. Am. Soc. Echocardiogr.* 19(7), 839–847 (2006).

48   Chan J, Hanekom L, Wong C *et al.*: Differentiation of subendocardial and transmural infarction using two-dimensional strain rate imaging to assess short-axis and long-axis myocardial function. *J. Am. Coll. Cardiol.* 48(10), 2026–2033 (2006).

49   Voigt JU, Exner B, Schmiedehausen K *et al.*: Strain-rate imaging during dobutamine stress echocardiography provides objective evidence of inducible ischemia. *Circulation* 107, 2120–2126 (2003).

50   Jamal F, Strotmann J, Weidemann F *et al.*: Noninvasive quantification of the contractile reserve of stunned myocardium by ultrasonic strain rate and strain. *Circulation* 104(9), 1059–1065 (2001).

51   Hoffmann R, Altiok E, Nowak B *et al.*: Strain rate measurement by Doppler echocardiography allows improved assessment of myocardial viability inpatients with depressed left ventricular function. *J. Am. Coll. Cardiol.* 39, 443–449 (2002).

52   Hanekom L, Jenkins C, Short L, Marwick TH: Accuracy of strain rate techniques for identification of viability at dobutamine stress echo: a follow-up study after revascularization. *Circulation* 112, 3892–3900 (2005).

53   Fathi R, Cain P, Nakatani S, Yu HC, Marwick TH: Effect of tissue Doppler on the accuracy of novice and expert interpreters of dobutamine echocardiography *Am. J. Cardiol.* 88, 400–405 (2001).

54   Davidavicius G, Kowalski M, Williams RI *et al.*: Can regional strain and strain rate measurement be performed during both dobutamine and exercise echocardiography, and do regional deformation responses differ with different forms of stress testing? *J. Am. Soc. Echocardiogr.* 16, 299–308 (2003).

55   Marciniak M, Claus P, Streb W *et al.*: The quantification of dipyridamole induced changes in regional deformation in normal, stunned or infarcted myocardium as measured by strain and strain rate: an experimental study. *Int. J. Cardiovasc. Imaging* 24(4), 365–376 (2008).

56   Dandel M, Hetzer R: Echocardiographic strain and strain rate imaging – clinical applications. *Int. J. Cardiol.* 132, 11–24 (2009).

57   Herbots L, D'hooge J, Eroglu E *et al.*: Improved regional function after autologous bone marrow-derived stem cell transfer in patients with acute myocardial infarction: a randomized, double-blind strain rate imaging study. *Eur. Heart J.* 30(6), 662–670 (2009).

58   Ganame J, Mertens L, Eidem BW *et al.*: Regional myocardial deformation in children with hypertrophic cardiomyopathy: morphological and clinical correlations. *Eur. Heart J.* 28(23), 2886–2894 (2007).

59   Saghir M, Areces M, Makan M: Strain rate imaging differentiates hypertensive cardiac hypertrophy from physiologic cardiac hypertrohy (athlete's heart). *J. Am. Soc. Echocardiogr.* 20(2), 151–157 (2007).

60   Kato TS, Noda A, Izawa H *et al.*: Discrimination of nonobstructive hypertrophic cardiomyopathy from hypertensive left ventricular hypertrophy on the basis of strain rate imaging by tissue Dopper ultrasonography. *Circulation* 110, 3808–3814 (2004).

61   Ganame J, Pignatelli RH, Eidem BW *et al.*: Myocardial deformation abnormalities in pediatric hypertrophic cardiomyopathy: are all etiologies identical? *Eur. J. Echocardiogr.* 9(6), 784–790 (2008).

62   Plaksej R, Kosmala W, Frantz S *et al.*: Relation of circulating markers of fibrosis and progression of left and right ventricular dysfunction in hypertensive patients with heart failure. *J. Hypertens.* 27(12), 2483–2491 (2009).

63   Weidemann F, Niemann M, Herrmann S *et al.*: A new echocardiographic approach for the detection of non-ischaemic fibrosis in hypertrophic myocardium. *Eur. Heart J.* 28, 3020–3026 (2007).

64   Koyama J, Ray-Sequin PA, Falk RH *et al.*: Longitudinal myocardial function assessed by tissue velocity, strain and strain rate tissue Doppler echocardiography in patients with AL (primary) cardiac amyloidosis. *Circulation* 107, 2446–2452 (2003).

65   Bellavia D, Abraham TP, Pellikka PA *et al.*: Detection of left ventricular systolic dysfunction in cardiac amyloidosis with strain rate echocardiography. *J. Am. Soc. Echocardiogr.* 20(10), 1194–1202 (2007).

66   Hamdy AM: Use of strain and tissue velocity imaging for early detection of regional myocardial dysfunction in patients with β-thalassemia. *Eur. J. Echocardiogr.* 8, 102–109 (2007).

67   Weidemann F, Eyskens B, Mertens L *et al.*: Quantification of regional right and left ventricular function by ultrasonic strain and strain rate indexes in Friedreich's ataxia. *Am. J. Cardiol.* 91, 622–626 (2003).

68   Fang ZY, Schull-Meade R, Downey M *et al.*: Determinants of subclinical diabetic heart disease. *Diabetologia* 48, 394–402 (2005).

69   Mertens L, Ganame J, Claus P *et al.*: Early regional myocardial dysfunction in young patients with Duchenne muscular dystrophy. *J. Am. Soc. Echocardiogr.* 21(9), 1049–1054 (2008).

70   Ganame J, Claus P, Eyskens B *et al.*: Acute cardiac functional and morphological changes after Anthracycline infusions in children. *Am. J. Cardiol.* 99(7), 974–977 (2007).

71   Jurcut R, Wildiers H, Ganame J *et al.*: Strain rate imaging detects early cardiac effects of pegylated liposomal Doxorubicin as adjuvant therapy in elderly patients with breast cancer. *J. Am. Soc. Echocardiogr.* 21(12), 1283–1289 (2008).

72   Migrino RQ, Aggarwal D, Konorev E *et al.*: Early detection of doxorubicin cardiomyopathy using two-dimensional strain echocardiography. *Ultrasound Med. Biol.* 32(4), 208–214 (2008).

73   Marciniak A, Sutherland GR, Marciniak M *et al.*: Myocardial deformation abnormalities in patients with aortic regurgitation: a strain rate imaging study. *Eur. J. Echocardiogr.* 10(1), 112–119 (2009).

74   Marciniak A, Claus P, Sutherland GR *et al.*: Changes in systolic left ventricular function in isolated mitral regurgitation. A strain rate imaging study. *Eur. Heart J.* 28(21), 2627–2636 (2007).

75   Lee R, Hanekom L, Marwick TH *et al.*: Prediction of subclinical left ventricular dysfunction with strain rate imaging in patients with asymphomatic severe mitral regurgitation. *Am. J. Cardiol.* 94, 1333–1337 (2004).

76   Kowalski M, Herbots L, Weidemann F *et al.*: One-dimensional ultrasonic strain and strain rate imaging: a new approach to the quantitation of regional myocardial function in patients with aortic stenosis. *Ultrasound Med. Biol.* 29(8), 1085–1092 (2003).

77   Bauer F, Eltchaninoff H, Tron C *et al.*: Acute improvement in global and regional left ventricular systolic function after percutaneous heart valve implantation in patients with symptomatic aortic stenosis. *Circulation* 110, 1473–1476 (2004).

78   Poulsen SH, Sogaard P, Nielsen-Kudsk JE, Egeblad H: Recovery of left ventricular systolic longitudinal strain after valve replacement in aortic stenosis and relation to natriuretic peptide. *J. Am. Soc. Echocardiogr.* 20(7), 877–884 (2007).

79   Dambrauskaite V, Delcroix M, Claus P *et al.*: Regional right ventricular dysfunction in chronic pulmonary hypertension. *J. Am. Soc. Echocardiogr.* 20(10), 1172–1180 (2007).

80   Huez S, Vachiéry JL, Unger P *et al.*: Tissue Doppler imaging evaluation of cardiac adaptation in severe pulmonary hypertension. *Am. J. Cardiol.* 100(9), 1473–1478 (2007).

81   Giusca S, Dambrauskaite V, Scheurwegs C *et al.*: Deformation imaging describes RV function better than longitudinal displacement of the tricuspid ring (TAPSE). *Heart* 96(4), 281–288 (2009).

82   Prakasa KR, Wang J, Tandri H *et al.*: Utility of tissue Doppler and strain echocardiography in arrhythmogenic right ventricular dysplasia/cardiomyopathy. *Am. J. Cardiol.* 100(9), 1473–1478 (2007).

83   Nagueh SF, Middleton KJ, Kopelen HA *et al.*: Doppler tissue imaging: a noninvasive technique for evaluation of left ventricular relaxation and estimation of filling pressures. *J. Am. Coll. Cardiol.* 30, 1527–1533 (1997).

84   Ommen SR, Nishimura RA, Appleton CP *et al.*: Clinical utility of Doppler echocardiography and tissue Doppler imaging in the estimation of left ventricular filling pressures: a comparative simultaneous Doppler-catheterization study. *Circulation* 102, 1788–1794 (2000).

85   Voigt JU, Lindenmeier G, Werner D *et al.*: Strain rate imaging for the assessment of preload-dependent changes in regional left ventricular diastolic longitudinal function. *J. Am. Soc. Echocardiogr.* 15, 13–19 (2002).

86   Stoylen A, Skjelvan G, Skjaerpe T: Flow propagation velocity is not a simple index of diastolic function in early filling. A comparative study of early diastolic strain rate and strain rate propagation, flow and flow rate propagation in normal and reduced diastolic function. *Cardiovas. Ultrasound* 1, 3 (2003).

87   Dong SJ, Hees PS, Siu CO, Weiss JL, Shapiro EP: MRI assessment of LV relaxation by untwisting rate: a new isovolumic phase measure of tau. *Am. J. Physiol. Heart Circ. Physiol.* 281, H2002–H2009 (2001).

88   Notomi Y, Popovic ZB, Yamada H *et al.*: Ventricular untwisting: a temporal link between left ventricular relaxation and suction. *Am. J. Physiol. Heart Circ. Physiol.* 294(1), H505–H513 (2008).

89 Wakami K, Ohte N, Asada K *et al.*: Correlation between left ventricular end-diastolic pressure and peak left atrial wall strain during left ventricular systole. *J. Am. Soc. Echocardiogr.* 22, 847–851 (2009).

90 Balbataeva A, Marciniak M, Bijnens B *et al.*: How to detect early left atrial remodelling and dysfunction in mild-to-moderate hypertension. *J. Hypertens.* 27(10), 2086–2093 (2009).

91 Di Salvo G, Caso P, Piccolo RL *et al.*: Atrial myocardial deformation properties predict maintenance of sinus rhythm after external cardioversion of recent-onsent lone atrial fibrillation: a color doppler myocardial imaging and transthoracic and transesophageal echocardiographic study. *Circulation* 112, 387–395 (2005).

92 Wang T, Wang M, Fung JWH *et al.*: Atrial strain rate echocardiography can predict success or failure of cardioversion for atrial fibrilation: a combined transthoracic tissue Doppler and transesophageal imaging study. *Int. J. Cardiol.* 114, 202–209 (2007).

93 Schneider C, Malisius R, Krause K *et al.*: Strain rate imaging for functional quantification of the left atrium: atrial deformation predicts the maintenance of sinus rhythm after catheter ablation of atrial fibrillation. *Eur. Heart J.* 29, 1397–1409 (2008).

94 Friedberg MK, Silverman NH, Dubin AM, Rosenthal DN: Mechanical dyssynchrony in children with systolic dysfunction secondary to cardiomyopathy: a Doppler tissue and vector velocity imaging study. *J. Am. Soc. Echocardiogr.* 20(6), 756–763 (2007).

95 Knebel F, Schattke S, Bondke H *et al.*: Evaluation of longitudinal and radial two-dimensional strain imaging versus Doppler tissue echocardiography in predicting long-term response to cardiac resynchronization therapy. *J. Am. Soc. Echocardiogr.* 20(4), 335–341 (2007).

96 Tanaka H, Hara H, Saba S, Gorcsan J 3rd: Prediction of response to cardiac resynchronization therapy by speckle

tracking echocardiography using different software approaches. *J. Am. Soc. Echocardiogr.* 22(6), 677–684 (2009).

97 Yu CM, Gorcsan J 3rd, Bleeker GB *et al.*: Usefulness of tissue Doppler velocity and strain dyssynchrony for predicting left ventricular reverse remodeling response after cardiac resynchronization therapy. *Am. J. Cardiol.* 100(8), 1263–1270 (2007).

98 Gorcsan J 3rd, Suffoletto MS: The role of tissue Doppler and strain imaging in predicting response to CRT. *Europace* 10(Suppl. 3), iii80–iii87 (2008).

99 Hawkins NM, Petrie MC, Burgess MI, McMurray JJ: Selecting patients for cardiac resynchronization therapy: the fallacy of echocardiographic dyssynchrony. *J. Am. Coll. Cardiol.* 53(21), 1944–1959 (2009).

100 Chung ES, Leon AR, Tavazzi L *et al.*: Results of the Predictors of Response to CRT (PROSPECT) Trial. *Circulation* 117, 2608–2616 (2008).

101 Parsai C, Bijnens B, Sutherland GR *et al.*: Toward undersatnding response to cardiac resynchronization therapy: left ventricular dyssynchrony is only one of multiple mechanisms. *Eur. Heart J.* 30, 940–949 (2009).

102 Voigt JU, Schneider TM, Korder S *et al.*: Apical transverse motion as surrogate parameter to determine regional left ventricular function inhomogeneities: a new, integrative approach to left ventricular asynchrony assessment. *Eur. Heart J.* 30(8), 959–968 (2009).

103 Popovic ZB, Grimm RA, Ahmad A *et al.*: Longitudinal rotation: an unrecognised motion pattern in patients with dilated cardiomyopathy. *Heart* 94(3), e11 (2008).

104 Dandel M, Weng Y, Siniawski H *et al.*: Long-term results in patients with idiopathic dilated cardiomyopathy after weaning from left ventricular assist devices. *Circulation* 112(Suppl. 9), I37–I45 (2005).

105 Dandel M, Hummel M, Müller J *et al.*: Reliability of tissue Doppler Wall motion monitoring after heart transplantation for replacement of invasive routine screenings by optimally timed cardiac biopsies and catheterizations. *Circulation* 104(12 Suppl. 1), I184–I191 (2001).

106 Dandel M, Wellnhofer E, Hummel M *et al.*: Early detection of left ventricular dysfunction related to transplant coronary artery disease. *J. Heart Lung Tranplant* 22, 1353–1364 (2003).

107 Eroglu E, D'hooge J, Sutherland GR *et al.*: Quantitative dobutamine stress echocardiography for the early detection of cardiac allograft vasculopathy in heart transplant recipients. *Heart* 94(2), e3 (2008).

108 Marciniak A, Eroglu E, Marciniak M *et al.*: The potential clinical role of ultrasonic strain and strain rate imaging in diagnosing acute rejection after heart transplantation. *Eur. J. Echocardiogr.* 8(3), 213–221 (2007).

109 Crosby J, Amundsen BH, Hergum T, Remme EW, Langeland S, Torp H: 3D speckle tracking for assessment of regional left ventricular function. *Ultrasound Med. Biol.* 35(3), 458–471 (2009).

110 Elen A, Choi HF, Loeckx D *et al.*: 3D cardiac strain estimation using spatio-temporal elastic registration of ultrasound images: a feasibility study. *IEEE Trans. Med. Imaging* 27(11), 1580–1591 (2008).

111 Perez de Isla L, Balcones DV, Fernández-Golfín C *et al.*: Three-dimensional-wall motion tracking: a new and faster tool for myocardial strain assessment: comparison with two-dimensional-wall motion tracking. *J. Am. Soc. Echocardiogr.* 22(4), 325–330 (2009).

112 Saito K, Okura H, Watanabe N *et al.*: Comprehensive evaluation of left ventricular strain using speckle tracking echocardiography in normal adults: comparison of three-dimensional and two-dimensional approaches. *J. Am. Soc. Echocardiogr.* 22(9), 1025–1030 (2009).

■ Website

201 Stoylen A: Introduction to strain and strain rate imaging of the heart for the novice researcher and curious clinician http://folk.ntnu.no/stoylen/strainrate

▪ Gives very good and didactic illustrations on the concepts and principles of ultrasound-based deformation estimation of the heart.